Detectability of Nonlinear Gravitational Wave Memory

Darin C. Mumma[1]
Mentors: Alan J. Weinstein[2], Colm Talbot[2], and Alvin K. Y. Li[2]
[1]*Departments of Physics and Philosophy, Grove City College, Grove City, PA 16127, US and*
[2]*LIGO Laboratory, California Institute of Technology, Pasadena, CA 91125, US*
(Dated: June 1, 2020)

Gravitational waves incident on an interferometer causes permanent distortion on the order of 10^{-21}-m, the so-called memory effect. Linear and nonlinear components exist in gravitational wave memory, the latter appearing as a non-oscillatory, cumulative signal. Current gravitational wave detectors are unable to reliably detect and isolate this low-frequency, nonlinear component which skews the numerical inferences of gravitational wave source parameters. Because this effect is cumulative, it is non-negligible, and its non-oscillatory nature distinguishes it from the rest of the waveform, making it detectable, in theory. Though previous studies have quantified and suggested improvements for the detectability of nonlinear memory, more templates and new data are available than ever before. In this project, we apply Bayesian parameter estimation to simulated compact binary coalescences with injected memory to determine nonlinear memory detectability.

I. INTRODUCTION

Although all accelerating masses radiate gravitational waves, compact binary coalescences – binary systems consisting of black holes and/or neutron stars – are especially interesting because they emit the most detectable gravitational wave signals and many of their properties are unknown. Indeed, the amplitude and phase of a gravitational wave encodes source features such as mass, angular momentum, and location. The traditional waveform sourced from a compact binary coalescence is an oscillatory traveling wave with increasing frequency and momentary amplitude spike corresponding to the merger phase. As it propagates through spacetime, this waveform distorts surrounding mass arrangements in an oscillating pattern, but afterwards each arrangement returns to its original geometry. However, general relativity predicts that after a gravitational wave passes a truly free-falling arrangement of masses, a memory effect occurs in which a permanent nonzero difference in deformation is observed [1–3]. Further, all gravitational waves possess some form of memory, whether linear or nonlinear.

Linear memory arises from non-oscillating masses and, thus, usually appears only in systems with hyperbolic orbits, neutrino ejection, or gamma-ray bursts. Nonlinear memory arises from the signal contribution of secondary gravitational waves sourced by the initial wave emission. Unlike non-oscillating masses, secondary gravitational wave production occurs in many compact binary coalescences, making nonlinear memory of especially prominence. Also, nonlinear memory accumulates over time because it is hereditary – depends on the entire past motion of the source. The non-oscillating and cumulative nature of nonlinear memory should, in theory, make it easy to distinguish from a normal gravitational wave signal [4]. In practice this is not the case.

There are two main reasons why nonlinear memory is, in fact, hard to extract from a gravitational wave signal. Current detectors are attuned to high-frequency input and are thus insensitive to nonlinear memory because the detector response is generally much shorter than the time over which the memory accumulates. Also, ground-based detectors are incapable of storing the memory over an extended period of time because electrostatic forces exist between adjoining particles throughout the detector, quickly eradicating the memory effect from early portions of the signal. This often lowers the observed memory effect below the resolution of the detectors.

Even without considering memory, overall detector data is very noisy. The primary goal of gravitational wave signal analysis is to distinguish actual signals from this background noise. All phases of compact binary coalescence-sourced waveforms are well-modeled using numerical simulations, allowing a template library to be constructed over a broad range of binary component masses and spins. Matched filtering can then be used to compare these templates with the data and determine the best fit. When nonlinear gravitational wave memory enters the picture, this same process can also be used to determine the detectability of the memory contribution by comparing the template's memory with measured memory.

From here, we discuss the theoretical background behind gravitational waves, matched filtering, nonlinear memory, and parameter estimation in Section II. In Section III, we summarize the procedure involved in determining memory detectability. Finally, Section IV features the work plan for the project.

II. BACKGROUND

A. Gravitational Wave Theory and Detection

An implication of Einstein's general relativity is that black holes, neutron stars, and other massive objects accelerating in spacetime generate ripples known as gravitational waves [5]. Here we will discuss the speed and polarizations of gravitational waves as well as instruments and methods used to detect them.

1. Speed of gravity

General relativity predicts that gravitational waves propagate at the speed of light [5], and several measurements have

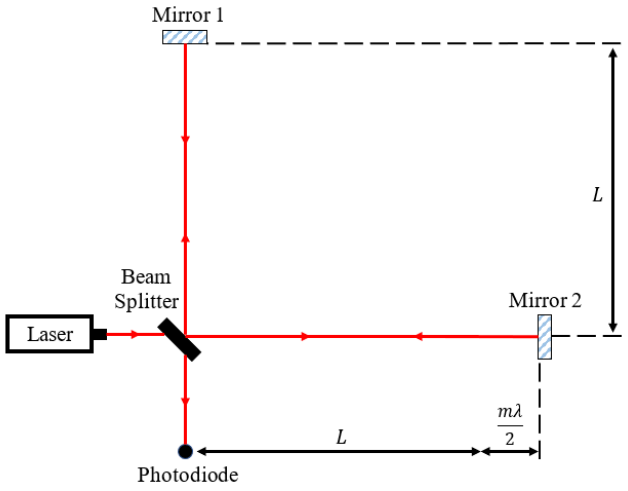

Figure 1. Simplified diagram of a standard LIGO detector.

been made to confirm this prediction using LIGO data. Most notably, Cornish *et al* [6] and Liu *et al* [7] used the difference in arrival time across multiple gravitational wave detectors during the second LIGO observing run to accurately measure each signal's speed. The first experimenter was able to constrain gravity's speed to within 20% of c and the second was able to constrain it to within only 3% of c.

2. *Gravitational wave polarizations and detectors*

Another prediction of general relativity is that passing spacetime ripples distort surrounding masses in an oscillatory manner, creating a variable strain on extended bodies. The frequency and amplitude of the oscillations are related to the angular momentum and mass of the ripple's source, respectively [8]. A Michelson-Morley interferometer may be used to record these variations in strain: two arms are set perpendicular to one another, and a laser and beamsplitter are arranged at the intersection point as shown in Figure (1). The laser is fired through the beamsplitter, creating two beams which travel along each arm and return after reflecting from mirrors placed at the end of each arm. Both beam paths are aligned to recombine at a photodiode located at the intersection point. Before a gravitational passes through, the only phase difference which exists between both beams arises from the difference in arm length, which is carefully adjusted to produce destructive interference at the photodiode.

However, both arm lengths are changed oppositely to one another by a passing gravitational wave, altering the phase difference and, thus, combined intensity of the light incident on the photodiode. This intensity information may be translated to strain information which is given in Equation (1)

$$h_{ij}(t,\,\mathbf{r}) = \sum_{A=+,\times} e^{A}_{ij}(\hat{\mathbf{n}}) \int_{-\infty}^{+\infty} h_A(f) e^{-i2\pi f\left(t-\frac{\hat{\mathbf{n}}\cdot\mathbf{r}}{c}\right)}\, dt. \qquad (1)$$

In general relativity, the spacetime metric is transverse-traceless gauge invariant, implying that free-falling objects are at rest in spacetime. So, if earth-based interferometers are in free-fall, Equation (1) is independent of $\mathbf{r}$, which may thus be set to 0. This yields the expression given in Equation (2)

$$h_{ij}(t) = \sum_{A=+,\times} e^{A}_{ij}(\hat{\mathbf{n}}) h_A(t), \qquad (2)$$

which clearly expresses the total strain as a sum of two linear polarizations, plus and cross. Plus polarized gravitational waves incident on a detector stretch and squeeze the arms directly along their length while cross polarized gravitational waves alter each arm's length at a 45° angle as shown in Figure (2). Generally, incident gravitational waves are a combination of these two polarizations or even of nonlinear polarizations.

3. *Signal types and detection methods*

To date, there are multiple gravitational wave types which have been detected including continuous, stochastic, burst, and compact binary coalescence gravitational waves. Continuous gravitational waves are radiated by spinning neutron stars and thus maintain constant frequency and amplitude. Stochastic gravitational waves likely come from especially distant sources and thus arrive in random patterns and are relatively insignificant in strength. Burst gravitational waves are unpredicted and currently unexplained but nevertheless exist as short duration, large amplitude pulses. Relevant to this paper, compact binary coalescence gravitational waves are sourced from inspiraling compact objects, such as black holes and/or neutron stars, and thus vary in frequency and amplitude over time. Compact binary coalescences consist of three phases, including an inspiral, merger, and ringdown as shown in Figure (3). In the inspiraling stage, the separation distance and rotation period of the binary components decay due to radiated energy in the form of gravitational waves. This portion of the signal increases in frequency and amplitude as the merger approaches. In the merger phase, the signal's amplitude briefly spikes as the binary components combine. In the ringdown stage, the resulting component stabilizes, producing a signal with decreasing frequency and amplitude. Among these four types of gravitational waves, compact binary coalescence gravitational waves have the most well-modeled waveforms.

Increased detector sensitivity is achieved by equally extending both beam paths through the careful arrangement of mirrors which allow multiple reflections to take place before the beams are recombined. As a result, typical detector sensitivity allows for measurements of strain on the order of 10^{-18}-m. However, this high sensitivity to shifting masses makes it hard

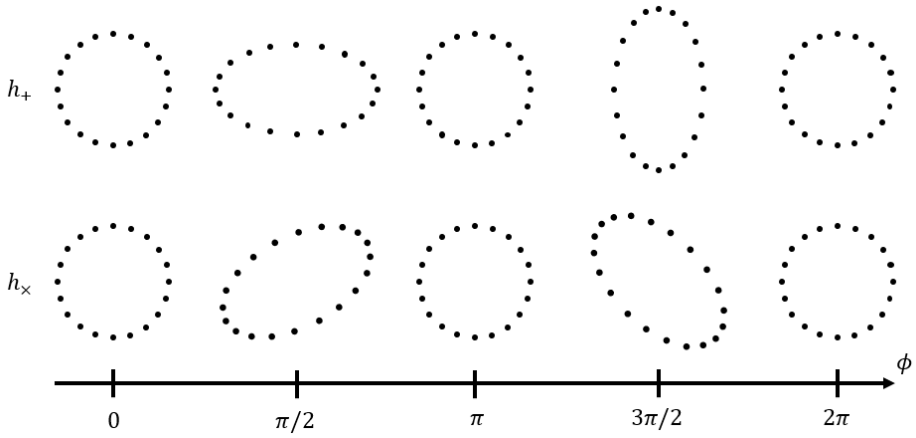

Figure 2. Linear polarizations of a gravitational wave illustrated over a complete phase cycle. Each dot represents a distinct test mass.

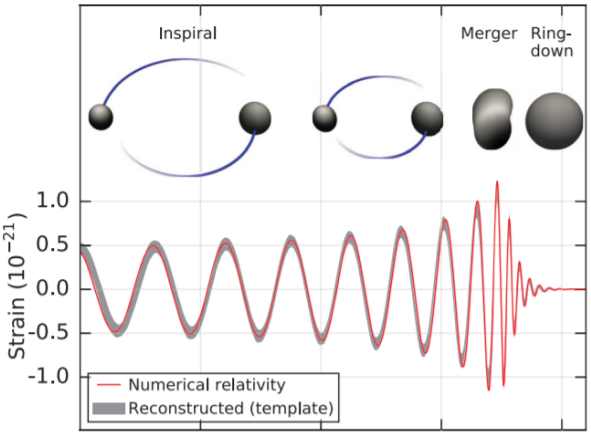

Figure 3. Compact binary coalescence gravitational-wave strain amplitude that shows the full bandwidth of a typical waveform. The inset images show the inspiral, merger, and ringdown phases of two coalescing objects. Retrieved from Abbott *et al* [9].

to distinguish between gravitational wave signals and background noise. This noise is often both local and non-local, frequently masking or even mimicking gravitational wave signals. Random noise is due to local causes and is thus uncorrelated among an array of distant detectors, whereas a passing gravitational wave is incident on every point of the earth nearly simultaneously. So, comparison of data among multiple detectors may be used to distinguish real signals from random signals. However, non-local events such as gamma ray passage, earthquakes, and ocean waves may also be picked up by the detector and cannot be removed by comparison of multiple detector's data. Instead, such noise is identified and extracted by comparing real time data from seismographs, microphones, and gamma ray detectors to LIGO's data. Identifying gravitational waves is further improved by comparing data to numerical templates constructed according to general relativity. This process, known as matched filtering, is explained in the next section.

B. Matched Filtering

The specifics of parameter estimation in determining memory detectability is mostly matched filtering. Here we will start by describing this process without memory and then include memory afterwards.

1. *Matched filtering without memory*

The ability to extract a signal from background noise is given by the signal-to-noise ratio, ρ, which is typically low, and matched filtering is a process by which it may be maximized. In matched filtering, templates are cross-correlated with observed data in frequency space to see if the resulting amplitude spikes occur at the known frequencies contained in a given template. If the frequencies match, the parameters, identity, and waveform of the template source is taken to be those of the signal source as well. However, the overwhelming presence of noise in the data makes a direct application of this process impossible. First, a filter must be matched with each template to maximize the signal-to-noise ratio for all cross-correlations.

To accomplish this for a given template, the template signal is injected into typical noise and the result is cross-correlated with the initial template adjusted in some initially unknown way to maximize the signal-to-noise ratio. The cross-correlation is given in Equation (3)

$$\hat{s} \propto \int_0^T s(t)K(t)\,dt, \tag{3}$$

where T is the observing time, $s(t)$ is the injected signal plus noise, and $K(t)$ is the adjusted template signal. Formally, $\rho = S/N$,where S is the expectation value of $\hat{s}$ with an injected signal, and N is the root mean square value of $\hat{s}$ when no signal is present. So, the goal is to select a $K(f)$ in the frequency domain which maximizes Equation (3) across the signal's frequency band, maximizing ρ. This $K(f)$ then becomes a given

template's filter function and is cross-correlated with real data in frequency space as if it were the correct fit for the hidden signal. According to this assumption, the extracted frequencies at which ρ is at maximum value are the signal's frequency band: all other frequencies included in the data are inhabited only by noise. These extraneous frequencies are thus removed from the data, and, if the template actually matches the hidden signal, the peak existing at the target frequency band will now extend far above the noise. If no such peak exists, the process is repeated using other templates.

Two difficulties with the matched filtering process exist. Firstly, since the presence and waveform of a gravitational wave signal are unknown prior to the matched filtering process, the noise is often difficult to characterize. But ρ depends on S and N, and thus requires knowledge of the signal and background noise. Secondly, an assembly of templates is necessarily discrete, making even correctly-chosen templates an approximation and thus lowering ρ from its value in the filter preparation stage. Consequently, a threshold ρ must be set below a given template's ideal ρ, and a template which achieves values above this threshold identifies and characterizes the hidden gravitational wave. This process is enhanced by combining data from multiple detectors to increase ρ as given in Equation (4)

$$\rho_{net}^2 = \sum_i \rho_i^2, \tag{4}$$

where i runs over each detector.

2. *Matched filtering with memory*

Matched filtering can also be used to determine the detectability of the memory contribution. In this case, a template with known memory is injected into a typical noise distribution and extracted using matched filtering. The difference between the overall template signal and extracted signal determines the measured memory effect. Comparison between the known and measured values yields a given interferometer's memory detectability.

C. Nonlinear Memory Theory

The non-linear (Christodoulou) gravitational wave memory is a permanent displacement of freely-falling test masses due to the passage of gravitational waves [4]. According to general relativity, a post-Newtonian expansion exists in which non-linear memory is described by terms which immediately follow the primary waveform and linear memory. However, far from being negligible, these terms accumulate memory over the duration of the signal, increasing most rapidly during the merger. These increasing terms arise from the signal contribution of secondary gravitational waves sourced by the primary waveform, and can thus be viewed as linear memory from waves which began from an arbitrary point in spacetime. Comparison between memory with and without a non-linear component is shown in Figure (4) for plus and cross polarized signals and across a variety of mass and spin combinations. In most combinations, the non-linear component is readily seen to be substantial.

The strength of non-linear memory depends on incident angle in much the same way as the primary waveform and, as just mentioned, increases monotonically over time. It is clear, then, that non-linear memory has an angular and temporal dependence which vary independent of one another, suggesting separation of variables. Indeed, through an application of separation of variables and projection of the linear polarizations of the waveform onto the spherical harmonics, one yields

$$\delta h_{lm} = \frac{R}{4\pi c} \Gamma_{lm}^{l_1 l_2 m_1 m_2}(\Omega) H_{l_1 l_2 m_1 m_2}(T_0, T_F), \tag{5}$$

where l and m designate a spherical harmonic mode for each binary component, δh_{lm} is the overall non-linear memory for a given mode, $\Gamma_{lm}^{l_1 l_2 m_1 m_2}(\Omega)$ encodes the angular dependence of the memory, and $H_{l_1 l_2 m_1 m_2}(T_0, T_F)$ encodes the time dependence. $\Gamma_{lm}^{l_1 l_2 m_1 m_2}(\Omega)$ is a geometry factor closely related to the spherical harmonics and may thus be tabulated and inserted in advance before any experiment-specific calculations are made. $H_{l_1 l_2 m_1 m_2}(T_0, T_F)$ is closely related to the total intensity of the secondary waveforms and thus must be computed after each signal is collected and processed. Using Equation (5), a tabulation of the spherical harmonics, and a properly chosen region of interest in an incident signal, nonlinear memory may be calculated.

It should be noted that the memory given in Equation (5) holds only for an assembly of freely-falling test masses, and is thus not true of the long term distortion of the arms in each ground-based detector because of the restorative electrostatic force existing between atoms. This dampens the non-linear memory's contribution to the signal, raising the minimum sensitivity required to identify and measure non-linear memory.

Nevertheless, accurate identification and measurement of non-linear memory will allow comparison with models, potentially lending further support to general relativity. Also, this will allow non-linear memory to be extracted from gravitational waveforms which will increase the accuracy of source parameter measurements. With the recent conclusion of the third LIGO observing run, much current data is now available, allowing for the detectability of non-linear memory to be determined. From such a determination, the magnitude and nature of sensitivity improvements for each detector may be evaluated so non-linear memory can be effectively detected in future observing runs.

D. Bayesian Parameter Estimation

Let the hypothesis H be the statement, "nonlinear memory is present in the detector's data" and, further, let D be the detector's data. Then, $P(H \mid D)$ is the probability that nonlinear memory is present in the data given the data we have at hand, $P(D \mid H)$ is the likelihood that we will detect nonlinear memory given that nonlinear memory is, in fact, present, and

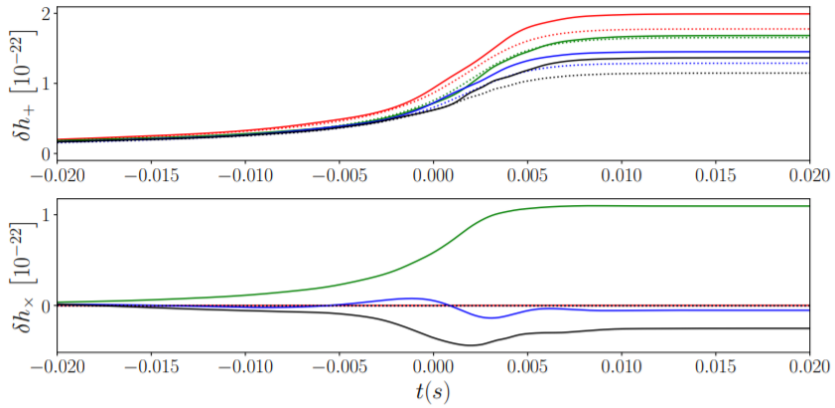

Figure 4. Including non-linear terms significantly affects the predicted memory. Comparison of the + (top panel) and × (bottom panel) polarizations of the memory time series when using only linear memory (dotted) and when using both linear and non-linear memory (solid). The colors are for binaries as follows: red is equal-mass with non-spinning components, green is equal-mass with precessing spins, blue is unequal mass with non-spinning components, black is unequal mass with precessing spins. In all cases, the late-time memory is different by at least 10% compared with the linear memory-only case and is larger for large mass ratios and precessing spins. Retrieved from Talbot *et al* [10].

$P(H)$ is the belief we have in the presence of nonlinear memory on the basis of prior information (or lack of information) alone. Bayes' Theorem relates these three quantities as shown in Equation (6).

$$P(H \mid D) \propto P(D \mid H) \times P(H) \tag{6}$$

Although we would eventually like to satisfy Equation (6) by determining $P(H \mid D)$, our present concern is finding $P(D \mid H)$, the likelihood or memory detectability.

The first step in parameter estimation is to present H as in Equation (7)

$$h_{tot} = h + \lambda h_{mem}, \tag{7}$$

where h_{tot} is the total signal, h is the non-memory portion of the signal, and h_{mem} is nonlinear memory. Then, for a template with known memory $\lambda = P(H)$ and is thus 1, but for the same template injected among noise, $\lambda = P(D \mid H)$ and can take on any value between 0 and 1. The value of this second λ is the memory detectability and values close to 1 indicate a high likelihood of memory detection whereas values close to 0 indicate a low likelihood of detection.

III. PROCEDURE

In this project, we will assess the detectability of memory in gravitational waves and subsequently search for methods to improve it. To achieve this goal, sufficient mastery of Bayesian parameter estimation, signal simulation, and python coding must be achieved. Here we will discuss the projected stages of the project.

Firstly, the primary author will become familiar with python and PyCBC, a python package containing algorithms that can detect coalescing compact binaries and measure gravitational wave parameters. General python competency will equip him with the required coding skills which will be necessary later in the project while PyCBC will acquaint him with the general shape of gravitational waveforms and how to generate them.

Secondly, the primary author will become familiar with the python package GWmemory, which calculates and constructs nonlinear memory waveforms from selected gravitational signals. Familiarity with this package will improve his understanding of memory effects on gravity wave signals and how to generate signals with memory.

Third, the primary author will acquire a better understanding of Bayesian inference and become familiar with BILBY, a python package which consists of inferencing tools for parameter estimation.

Fourthly, we will work on our primary goal by assessing the detectability of memory in gravitational waves. Equation (7) presents an all-or-nothing waveform model for gravitational waves with memory, where λ represents the memory constant. We will inject a signal with memory (i.e. $\lambda = 1$) into a typical noise distribution, and then apply matched filtering to extract the signal and infer the value of the memory constant. This inferred value represents the memory detectability, and a value close to 1 means we are able to identify memory in the signal, whereas smaller values indicate decreasing likelihood of identification.

Fifthly, given additional time, we will investigate methods by which the detectability of gravitational wave memory can be improved.

IV. WORK PLAN

A work plan has been included in Table I, listing weekly project goals for the Summer 2020 LIGO SURF project.

Table I. Work plan for the Summer 2020 LIGO SURF program. Schedule is broken down by week and projected progress.

Date	Progress
June 1	1. Deadline for submitting project proposal.
June 16	2. Start of LIGO SURF 2020.
June 16–20 (Week 1)	3. Understand basic python and PyCBC functionality.
June 21–27 (Week 2)	4. Increase ability to work with PyCBC.
July 28–July 4 (Week 3)	5. Continue working with PyCBC and begin familiarizing with GWmemory.
July 5–11 (Week 4)	6. Continue familiarizing with GWmemory. 7. Submit interim report 1.
July 12–18 (Week 5)	8. Begin learning BILBY.
July 19–25 (Week 6)	9. Continue learning BILBY and start main project.
July 26–August 1 (Week 7)	10. Main Project: Formation of effective work flow. 11. Submit interim report 2. 12. Submit abstract.
August 2–8 (Week 8)	13. Main Project: Produce results.
August 9–15 (Week 9)	14. Investigate detectability improvement.
August 16–21 (Week 10)	15. Continue investigating detectability improvement. 16. Final presentation.
September 28	17. Deadline for submitting final report.

[1] Y. B. Zeldovich and A. G. Polnarev. *Sov. Astron.*, 18(17), 1974.
[2] V. B. Braginsky and L. P. Grishchuk. *Sov. Phys. JETP*, 62(3): 427–430, 1985.
[3] V. B. Braginsky and K. S. Thorne. *Nature*, 327(6118):123–125, 1987.
[4] M. Favata. *Classical Quantum Gravity*, 27(8), 2010.
[5] A. Einstein. *Sitzungsber. Preuss. Akad. Wiss.*, 1:135–149, 1918.
[6] N. Cornish et al. *Phys. Rev. Lett.*, 119(16), 2017.
[7] X. Liu et al. *arXiv*, 2020.
[8] B. P. Abbott et al. *Phys. Rev. X*, 9(3), 2019.
[9] B. P. Abbott et al. *Phys. Rev. Lett.*, 116(6), 2016.
[10] C. Talbot et al. *Phys. Rev. D*, 98(6), 2018.